THE CURVELET TRANSFORM FOR IMAGE FUSION

Myungjin Choi [a] , Rae Young Kim [b,] *, Moon-Gyu Kim [a]

[a] SaTReC, [b] Division of Applied Mathematics , KAIST
373-1, Guseong-dong, Yuseong-gu, Daejeon, 305-701, Republic of KOREA
[a] (prime,mgkim)@satrec.kaist.ac.kr; [b] rykim@amath.kaist.ac.kr

KEY WORDS: Fusion, Multiresolution analysis, IKONOS, Wavelet transform, Curvelet transform

ABSTRACT:

The fusion of high-spectral but low spatial resolution multispectral and low-spectral but high spatial resolution panchromatic satellite images is a very useful technique in various applications of remote sensing. Recently, some studies showed that wavelet-based image fusion method provides high quality of the spectral content of the fused image. However, most of wavelet-based methods have a spatial resolution of the fused result less than the Brovey, IHS, and PCA fusion methods. In this paper, we introduce a new method based on the curvelet transform which represents edges better than wavelets. Since edges play a fundamental role in image understanding, one good way to enhance spatial resolution is to enhance the edges. Curvelet-based image fusion method provides richer information in the spatial and spectral domains simultaneously. We performed IKONOS image fusion. This new method has reached an optimum fusion result.

1. INTRODUCTION

In many remote sensing and mapping applications, the fusion of multispectral and panchromatic images is a very important issue.

Many image fusion techniques and software tools have been developed. The well-known methods are, for example, the Brovey, the IHS(Intensity, Hue, Saturation) color model, the PCA(Principal Components Analysis) method, and wavelet based method(Ranchin *et al*.2000).

Assessment of the quality of the fused images is another important issue. Wald et al. (1997) proposed an approach with criteria that can be used for evaluation the spectral quality of the fused satellite images.

If the objective of image fusion is to construct synthetic images that are closer to the reality they represent, then, according to the criteria proposed by Wald et al.(1997)., the Brovey, IHS, and PCA fusion methods meet this objective. However, one limitation of such methods is some distortion of spectral characteristics in the original multispectral images. Recently developments in wavelet analysis provide a potential solution to these drawbacks. For example, Nunez et al.(1999) developed an approach to fuse a high-resolution panchromatic image with a low-resolution multispectral image based on wavelet decomposition. Ranchin and Wald designed the ARSIS concept for fusing high spatial and spectral resolution images based on the multiresolution analysis of two-band wavelet transformation.

Wavelet-based image fusion method provides high spectral quality of the fused satellite images. However, the fused image by Wavelets have much less spatial information than those by the Brovey, IHS, and PCA methods. The spatial information of fused image is an important factor as much as the spectral information in many remote sensing applications. In particular, this improves the efficiency of the image fusion application, such as unsupervised image classification. In other words, it is necessary to develop advanced image fusion method so that the fused images have the same spectral resolution as the multispectral images and the same spatial resolution as the panchromatic image with minimum artifacts.

Recently, other multiscale systems have been developed, which include in particular ridgelets (Candes, 1999) and curvelets (Candes *et al*, 1999;Starck *et al*,2002), and these are very different from wavelet-like systems. Curvelets and ridgelets take the form of basis elements which exhibit very high directional sensitivity and are highly anisotropic. Therefore, the curvelet transform represents edges better than wavelets, and is well-suited for multiscale edge enhancement(Starck *et al*,2002).

In this paper, we introduce a new image fusion method based on the curvelet transform. The fused image using curvelet-based image fusion method represents almost the same detail as the original panchromatic image because curvelets represent edges better than wavelets, and the same colour as the original multispectral images because we use the wavelet-based image fusion method naturally in our algorithm. Therefore, this new method is an optimum method for image fusion. We develop a new approach for fusing IKONOS pan and multispectral images based on the curvelet transform.

The structure of this paper is as follows. The next section describes the theoretical basis of the ridgelets and curvelets. Then, a new image fusion approach for IKONOS pan and multispectral images based on the curvelet transform is presented. This is followed by a discussion of the image fusing experiments. Next, the experimental results are analysed. Furthermore, the proposed method is compare with the previous methods developed for image fusion, such as the wavelet method and the IHS method.

* The second author was supported by KRF-2002-070-C00004.

2. CONTINUOUS RIDGELET TRANSFORM

The two-dimensional continuous ridgelet transform in R^2 can be defined as follows(Candes, 1999; Starck *et al*, 2002). We pick a smooth univariate function $\psi:R\rightarrow R$ with sufficient decay and satisfying the admissibility condition

$$\int |\hat{\psi}(\xi)|^2 / |\xi|^2 \, d\xi < \infty \qquad (1)$$

which holds if, say, ψ has a vanishing mean $\int \psi(t)dt=0$. We will suppose that ψ is normalized so that $\int_0^\infty |\hat{\psi}(\xi)|^2 \xi^{-2} d\xi = 1$.

For each $a > 0$, each $b \in R$ and each $\theta \in [0, 2\pi)$, we define the bivariate ridgelet $\psi_{a,b,\theta} : R^2 \rightarrow R^2$ by

$$\psi_{a,b,\theta}(x) = a^{-1/2}\psi((x_1 \cos\theta + x_2 \sin\theta - b)/a) \qquad (2)$$

A ridgelet is constant along lines $x_1 \cos\theta + x_2 \sin\theta = const$. Transverse to these ridges it is a wavelet.

Given $f \in L^2(R^2)$, we define its ridgelet coefficients by

$$\Re_f(a,b,\theta) = \int \overline{\psi}_{a,b,\theta}(x) f(x) dx . \qquad (3)$$

If $f \in L^1(R^2) \cap L^2(R^2)$, then we have the exact reconstruction formula

$$f(x) = \int_0^{2\pi} \int_{-\infty}^{\infty} \int_0^{\infty} \Re_f(a,b,\theta)\psi_{a,b,\theta}(x) \frac{da}{a^3} db \frac{d\theta}{4\pi} . \qquad (4)$$

and a Parseval relation

$$\int |f(x)|^2 dx = \int_0^{2\pi} \int_{-\infty}^{\infty} \int_0^{\infty} |\Re_f(a,b,\theta)|^2 \frac{da}{a^3} db \frac{d\theta}{4\pi} . \qquad (5)$$

Hence, much like the wavelet or Fourier transforms, the identity (4) expresses the fact that one can represent any arbitrary function as a continuous superposition of ridgelets. Discrete analogs of (4) and (5) exists; see (Candes, 1999) or (Donoho, 2000) for a slightly different approach.

2.1 Radon Transform

A basic tool for calculating ridgelet coefficients is to view ridgelet analysis as a form of wavelet analysis in the Radon domain.

The Radon transform $R : L^2(R^2) \rightarrow L^2([0, 2\pi], L^2(R))$ is defined by

$$Rf(\theta,t) = \int f(x_1,x_2)\delta(x_1\cos\theta + x_2 \sin\theta - t)dx_1 dx_2 \qquad (6)$$

where δ is the Dirac distribution. The ridgelet coefficients $\Re_f(a,b,\theta)$ of an object f are given by analysis of the Radon transform via

$$\Re_f(a,b,\theta) = \int Rf(\theta,t) a^{-1/2} \psi((t-b)/a) dt \qquad (7)$$

Hence, the ridgelet transform is precisely the application of a 1-dimensional wavelet transform to the slices of the Radon transform where the angular variable θ is constant and t is varying.

2.2 Ridgelet Pyramids

Let Q denote a dyadic square $Q = [k_1/2^s, (k_1+1)/2^s) \times [k_2/2^s, (k_2+1)/2^s)$ and let Q be the collection of all such dyadic squares. We write Q_S for the collection of all dyadic squares of scale s. Associated to the squares $Q \in Q_S$ we construct a partition of energy as follows. With ω a nice smooth window obeying $\sum_{k_1,k_2} \omega^2(x_1-k_1, x_2-k_2)=1$, we dilate and transport ω to all squares Q at scale s, producing a collection of windows (ω_Q) such that the ω_Q^2s, $Q \in Q_S$, make up a partition of unity. We also let T_Q donote the transport operator acting on functions g via

$$(T_Q g)(x_1, x_2) = 2^s g(2^s x_1 - k_1, 2^s x_2 - k_2) .$$

With these notations, it is not hard to see that

$$f\omega_Q = \int < f, \omega_Q T_Q \psi_{a,b,\theta} > T_Q \psi_{a,b,\theta} \frac{da}{a^3} db \frac{d\theta}{4\pi} \qquad (8)$$

and, therefore, summing the above equalities across squares at a given scale gives

$$f = \sum_{Q \in Q_s} f\omega_Q^2 = \sum_Q \int < f, \omega_Q T_Q \psi_{a,b,\theta} > T_Q \psi_{a,b,\theta} \frac{da}{a^3} db \frac{d\theta}{4\pi} . \qquad (9)$$

The identity (9) expresses the fact that one can represent any function as a superposition of elements of the form $\omega_Q T_Q \psi_{a,b,\theta}$; that is, of ridgelet elements localized near the squares Q. For the function $T_Q \psi_{a,b,\theta}$ is the ridgelet ψ_{a_Q,b_Q,θ_Q} with parameters obeying

$$a_Q = 2^{-s} a , \quad b_Q = b + k_1 2^{-s} \cos\theta + k_2 2^{-s} \sin\theta , \quad \theta_Q = \theta$$

and, thus, $\omega_Q T_Q \psi_{a,b,\theta}$ is a windowed ridgelet, supported near the square Q, hence the name local ridgelet transform.

The previous paragraph discussed the construction of local ridgelets of fixed length, roughly 2^{-s} (s fixed). Letting the

scale s vary defines the multiscale ridgelet dictionary $\{\psi^{Q}_{a,b,\theta} : s \geq s_0, Q \in \mathrm{Q_S}, a > 0, b \in R, \theta \in [0, 2\pi)\}$ by

$$\psi^{Q}_{a,b,\theta} = \omega_Q T_Q \psi_{a,b,\theta}$$

that is, a whole pyramid of local ridgelets at various lengths and locations. This is, of course, a massively overcomplete representation system and no formula like (9) is available for this multiscale ridgelet pyramid, because it is highly overcomplete.

2.3 Discrete Ridgelet Transfrom(DRT)

A basic strategy for calculating the continuous ridgelet transform is first to compute the Radon transform $Rf(\theta, t)$ and second to apply a one-dimensional wavelet transform to the slices $Rf(\theta, \cdot)$.

A fundamental fact about the Radon transform is the projection-slice formula(Deans, 1983) :

$$\hat{f}(\omega\cos\theta, \omega\sin\theta) = \int Rf(\theta, t) e^{-2\pi i\omega t} dt \,. \qquad (10)$$

This says that the Radon transform can be obtained by applying the one-dimensional inverse Fourier transform to the two-dimensional Fourier transform restricted to radial lines through the origin.

This of course suggests that approximate Radon transforms for digital data can be based on discrete fast Fourier transforms. In outline, one simply does the following,

1. 2D-FFT
   Compute the two-dimensional Fast Fourier Transform (FFT) of f .
2. Cartesian to polar conversion
   Using an interpolation scheme, substitute the sampled values of the Fourier transform obtained on the square lattice with sampled values of $\hat{f}$ on a polar lattice: that is, on a lattice where the points fall on lines through the origin.
3. 1D-IFFT
   Compute the one-dimensional Inverse Fast Fourier Transform (IFFT) on each line; i.e., for each value of the angular parameter.

The use of this strategy in connection with ridgelet transform has been discussed in the articles(Deans, 1983 ; Donoho, 1998).

3. DIGITAL CURLET TRANSFORM

The idea of curvelets (Candes *et al*, 1999;Starck *et al*, 2002;Starck *et al*, 2003) is to represent a curve as a super-position of functions of various lengths and widths obeying the scaling law $width \approx length^2$. This can be done by first decomposing the image into subbands, i.e., separating the object into a series of disjoint scales. Each scale is then analysed by means of a local ridgelet transform.

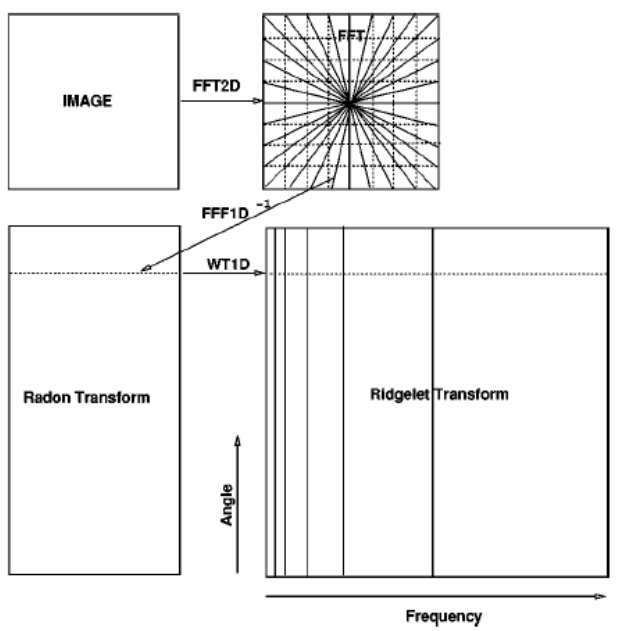

Figure 1. Ridgelet transform flowgraph. Each of the $2n$ radial lines in the Fourier domain is processed separately. The 1-D inverse FFT is calculated along each radial line followed by a 1-D nonorthogonal wavelet transform. In practice, the 1-D wavelet coefficients are directly calculated in the Fourier space.

Curvelets are based on multiscale ridgelets combined with a spatial bandpass filtering operation to isolate different scales. This spatial bandpass filter nearly kills all multiscale ridgelets which are not in the frequency range of the filter. In other words, a curvelet is a multiscale ridgelet which lives in a prescribed frequency band. The bandpass is set so that the curvelet length and width at fine scales are related by a scaling law $width \approx length^2$ and so the anisotropy increases with decreasing scale like a power law. There is very special relationship between the depth of the multiscale pyramid and the index of the dyadic subbands; the side length of the localizing windows is doubled at every other dyadic subband, hence maintaining the fundamental property of the curvelet transform which says that elements of length about $2^{-j/2}$ serve for the analysis and synthesis of the j th subband $[2^j, 2^{j+1}]$. While multiscale ridgelets have arbitrary dyadic length and arbitrary dyadic widths, curvelets have a scaling obeying $width \approx length^2$. Loosely speaking, the curvelet dictionary is a subset of the multiscale ridgelet dictionary, but which allows reconstruction.

The discrete curvelet transform of a continuum function $f(x_1, x_2)$ makes use of a dyadic sequence of scales, and a bank of filters $(P_0 f, \Delta_1 f, \Delta_2 f, \cdots)$ with the property that the passband filter Δ_s is concentrated near the frequencies $[2^{2s}, 2^{2s+2}]$, e.g.,

$$\Delta_s = \Psi_{2s} * f \,, \quad \hat{\Psi}_{2s}(\xi) = \hat{\Psi}(2^{-2s}\xi)$$

In wavelet theory, one uses a decomposition into dyadic subbands $[2^s, 2^{s+1}]$. In contrast, the subbands used in the

discrete curvelet transform of continuum functions have the non-standard form $[2^{2s}, 2^{2s+2}]$. This is non-standard feature of the discrete curvelet transform well worth remembering.

With the notations of section above, the curvelet decomposition is the sequence of the following steps.

- *Subband Decomposition*. The object f is decomposed into subbands

$$f \mapsto (P_0 f, \Delta_1 f, \Delta_2 f, \cdots).$$

- *Smooth Partitioning*. Each subband is smoothly windowed into "squares" of an appropriate scale (of sidelength $\approx 2^{-s}$)

$$\Delta_s f \mapsto (\omega_Q \Delta_s f)_{Q \in Q_S}$$

- *Renormalization*. Each resulting square is renormalized to unit scale

$$g_Q = (T_Q)^{-1}(\omega_Q \Delta_s f), \quad Q \in Q_S.$$

- *Ridgelet Analysis*. Each square is analysed via the discrete ridgelet transform.

In the definition, the two dyadic subbands $[2^{2s}, 2^{2s+1}]$ and $[2^{2s+1}, 2^{2s+2}]$ are merged before applying the ridgelet transform.

3.1 Digital Realization

In developing a transform for digital n by n data which is analogous to the discrete curvelet transform of a continuous function $f(x_1, x_2)$, we have to replace each of the continuum concepts with the appropriate digital concept mentioned in section above. Recently, Starck et al.(2002) showed that "`a trous" subband filtering algorithm is especially well-adapted to the needs of the digital curvelet transform. The algorithm decomposes an n by n image I as a superposition of the form

$$I(x, y) = c_J(x, y) + \sum_{j=1}^{J} \omega_j(x, y) \qquad (11)$$

where c_J is a coarse or smooth version of the original image I and ω_j represents "the details of I" at scale 2^{-j}, see (Starck *et al*, 1998) for more information. Thus, the algorithm outputs $J+1$ subband arrays of size $n \times n$. [The indexing is such that, here, $j = 1$ corresponds to the finest scale(high frequencies).]

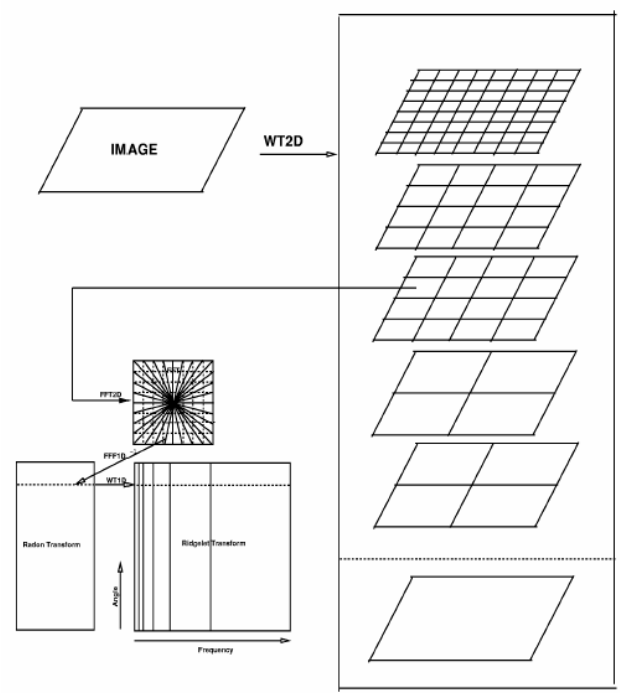

Figure 2. Curvelet transform flowgraph. The figure illustrates the decomposition of the original image into subbands followed by the spatial partitioning of each subband(i.e., each subband is decomposed into blocks). The ridgelet transform is then applied to each block .

3.2 Algorithm

Starck et al.(2002) presented a sketch of the discrete curvelet transform algorithm:

1) apply the `a trous algorithm with J scales;

2) set $B_1 = B_{\min}$;

3) for $j = 1, \ldots, J$ do

   a) partition the subband ω_j with a block size B_j and apply the digital ridgelet transform to each block;

   b) if j modulo 2 =1 then $B_{j+1} = 2B_j$;

   c) else $B_{j+1} = B_j$.

Note that the coarse description of the image c_J is not processed. Finally, Figure 2. gives an overview of the organization of the algorithm.

This implementation of the curvelet transform is also redundant. The redundancy factor is equal to $16J + 1$ whenever J scales are employed. Finally, the method enjoys exact reconstruction and stability, because this invertibility holds for each element of the processing chain.

4. THE IMAGE FUSION METHOD BASED ON THE CURVELET TRANSFORM

We now give the specific operational procedure for the proposed curvelet-based image fusion approach. The operational procedure is a generic one, although IKONOS images were taken as an example in order to illustrate the method.

(1) The original IKONOS pan and multispectral images are geometrically registered to each other.

(2) Three new IKONOS pan images I_1 , I_2 ,and I_3 are produced, whose histograms are specified according to the histograms of the multi-spectral images R, G, and B, respectively.

(3) By using well-known wavelet-based image fusion method, we obtained fused images I_1 +R, I_2 +G, and I_3 +B, respectively.

(4) I_1 , I_2 ,and I_3 are decomposed into $J+1$ subbands, respectively, by applying " `a trous" subband filtering algorithm. Each decomposed image includes c_J which is a coarse or smooth version of the original image and ω_j which represents "the details of I " at scale 2^{-j} .

(5) Each c_J is replaced by fused image which obtained from (3).

(6) The ridgelet transform is then applied to each block.

(7) Curvelet coefficients (or ridgelet coefficients) are modified in order to enhance edges in the fused image.

(8) The Curvelet reconstructions are carried out for I_1 , I_2 , and I_3 , respectively. Three new images (F_1 , F_2 , and F_3) are then obtained, which reflect the spectral information of the original multi-spectral images R, G, and B, and also the spatial information of the pan image.

(9) F_1 , F_2 , and F_3 are combined into a single fused image F .

In this approach, we can obtain an optimum fused image which has richer information in the spatial and spectral domains simultaneously. Therefore, we easily can find out small objects in the fused image and separate them. This is the reason why curvelets-based image fusion method is very efficient for image fusion.

5. EXPERIMENTAL STUDY AND ANALYSIS

5.1 Visual analysis

Since the curvelet transform is well-adapted to represent pan image containing edges and the wavelet transform preserves spectral information of original multispectral images, the fused image has high spatial and spectral resolution simultaneously.

From the fused image in Figure 3, it should be noted that both the spatial and the spectral resolutions have been enhanced, in comparison to the original images. The spectral information in the original panchromatic image has been increased, and the structural information in the original multispectral images has also been enriched. Hence, the fused image contains both the structural details of the higher spatial resolution panchromatic image and the rich spectral information from the multispectral images. Compared with the fused result by the wavelet, the fused result by the curvelets has a better visual effect in IKONOS image fusion in Figure 3.

(a) (b) (c)

Figure 3. (a) Original IKONOS colour images (b) Wavelet-based fusion result (c) Curvelet-based fusion result

5.2 Quantitative analysis

In addition to the visual analysis, we extended our investigation to a quantitative analysis. The experimental result was analysed based on the combination entropy, the mean gradient, and the correlation coefficient, as used in Shi et al.(2003).

Method	C.E	M.G	C.C
Original Images (R,G,B)	9.5632	20.9771 22.2667 21.6789	— — —
Image fused by Wavelet (F_1, F_2, F_3)	22.3452	22.7275 23.7696 23.9975	0.9261 0. 9196 0.8690
Image fused by Curvelet (F_1, F_2, F_3)	26.9948	25.8385 26.9576 28.4971	0.9457 0.9463 0.9289
Image fused by IHS (F_1, F_2, F_3)	16.5482	23.4475 23.6813 23.7283	0.9692 0.9951 0.9581

Table 1. A comparison of image fusion by the wavelets, the curvelets, and IHS methods.

Table 1 presents a comparison of the experimental results of image fusion using the curvelet-based image fusion method, the wavelet-based image fusion method, and IHS method in terms of combination entropy, the mean gradient, and the correlation coefficient.

The combination entropy (C.E.) represents the property of combination between images. The larger the combination entropy of an image, the richer the information contained in the image. In Table 1, the combination entropy of the curvelet-based image fusion is greater than those of other methods. Thus, the curvelet-based image fusion method is better than the wavelet and IHS methods in terms of combination entropy.

The mean gradient (M.G.) reflects the contrast between the details variation of pattern on the image and the clarity of the

image. And the correlation coefficient (C.C.) between the original and fused image shows the similarity in small size structures between the original and synthetic images. In Table 1, the mean gradient and the correlation coefficient of the curvelet-based image fusion method are grater than those of the wavelet-based image fusion method. As previously stated, if the object of image fusion is to construct synthetic images which are closer to the reality they represent, then the curvelet-based image fusion method meet this objective very well. This is one of the main advantages of using the curvelet transform for image fusion.

Based on the experimental results obtained from this study, the curvlet-based image fusion method is very efficient for fusing IKONOS images This new method has reached an optimum fusion result.

6. CONCLUSIONS

We have presented a newly developed method based on the curvelet transform for fusing IKONOS images. In this paper, an experimental study was conducted by applying the proposed method, and also other image fusion methods, for fusing IKONOS images. A comparison of the fused image from the wavelet and IHS method was made.

Based on the experimental results respecting the four indicators – the combination entropy, the mean gradient, and the correlation coefficient, the proposed method provides a good result, both visually and quantitatively, for remote sensing fusion.

ACKNOWLEDGEMENT

The first author much thanks Korea Aerospace Research Institute for providing the raw IKONOS images for this research.

References

Ranchin, T. and Wald, L., 2000. Fusion of High Spatial and Spectral Resolution images: The ARSIS Concept and Its Implementation. *Photogrammetric Engineering and Remote Sensing*, 66, pp. 49-61.

Wald, L., Ranchin, T., and Mangolini, M., 1997. Fusion of Satellite images of different spatial resolution: Assessing the quality of resulting images. *Photogrammetric Engineering and Remote Sensing*, 63(6), pp. 691-699.

Nunez, J., Otazu, X., Fors, O., Prades, A., Pala, V., and Arbiol, R., 1999. Multiresolution-based image fusion with addtive wavelet decomposion. *IEEE Transactions on Geoscience and Remote sensing*, 37(3), pp. 1204-1211.

Shi, W.Z., Zhu, C.Q., Zhu, C.Y., and Yang, X.M., 2003. Multi-Band Wavelet for Fusing SPOT Panchromatic and Multispectral Images. *Photogrammetric Engineering and Remote Sensing*, 69(5), pp. 513-520.

Candes, E. J., 1999. Harmonic analysis of neural networks. *Appl. Comput. Harmon. Anal.*, 6, pp. 197-218.

Candes, E. J., and Donoho, D. L., 1999. Curvelets- A surprisingly effective nonadaptie representation for objects with edges. in *Curve and Surface Fitting: Saint-Malo*, A. Cohen, C.Rabut, and L.L.Schumaker, Eds. Nashville, TN: Vanderbilt University Press.

Starck, J. L., Candes, E. J., and Donoho, D.L., 2002. The curvelet transform for image denosing. *IEEE Trans. Image Processing.*, 11, pp. 131-141.

Donoho, D.L., 2000. Orthonormal ridgelets and linear singularities. *SIAM J. Math Anal.*, 31(5), pp. 1062-1099.

Deans, S. R., 1983. The Radon transform and some of its applications. John Wiley Sons, New York.

Donoho, D. L., 1998. Digital ridgelet transform via rectopolar coordinate transform. Stanford Univ., Stanford, CA, Tech. Rep.

Starck, J. L., Murtagh, F., and Bijaoui, A., 1998. Image Processing and Data Analysis: The Multiscale Approach. Cambridge Univ. Press, Cambridge, U.K.

Starck, J. L., Candes, E. J., and Donoho, D.L., 2003. Gray and Color Image Contrast Enhancement by the Curvelet Transform. *IEEE Trans. Image Processing.*, 12(06), pp. 706-717.